




THE ACCURACY AND PRECISION OF SMALL-SIZED MODERN WOOD SAMPLES ANALYZED AT THE CHRONOS ¹⁴CARBON-CYCLE FACILITY

Heather A Haines^{1,2,3,4*}  • William T Hiscock^{3,4} • Jonathan G Palmer^{1,2,3,4}  • Chris S M Turney⁵ • Zoë A Thomas^{1,2,3,4}  • Haidee Cadd^{4,6,7} • Juee Vohra^{3,4} • Christopher E Marjo^{3,4}

¹School of Biological, Earth and Environmental Sciences, University of New South Wales (UNSW), NSW, 2052, Australia

²ARC Centre of Excellence for Australian Biodiversity and Heritage, UNSW Node, Australia

³Earth and Sustainability Science Research Centre (ESSRC), School of Biological, Earth and Environmental Sciences, University of New South Wales, Sydney, NSW, 2052, Australia

⁴Chronos ¹⁴Carbon-Cycle Facility, Mark Wainwright Analytical Centre, University of New South Wales, NSW, 2052, Australia

⁵Division of the Deputy Vice-Chancellor, Research, University of Technology Sydney, NSW, 2007, Australia

⁶School of Earth, Atmospheric and Life Sciences, University of Wollongong (UoW), NSW, 2522, Australia

⁷ARC Centre of Excellence for Australian Biodiversity and Heritage, UoW Node, Australia

ABSTRACT. Tree-ring series offer considerable potential for the development of environment-sensitive proxy records. However, with traditional increment cores, only small amounts of wood are often available from annual tree-ring sequences. For this reason, it is important to understand the reliability (and reproducibility) of radiocarbon measurements obtained from small-sized samples. Here we report the F¹⁴C results from the Chronos ¹⁴Carbon-Cycle Facility of modern tropical Australian tree samples over a range of four graphite target sizes from the same rings. Our study shows that similar precision can be obtained from full-sized, half-sized, as well as small-sized graphite targets using standard pretreatment and analysis procedures. However, with a decline in sample size, there was an increase seen in the associated variance of the ages and the smallest target weights started showing a systematic bias. Wiggle-matching accuracy tests, comparing the Southern Hemisphere post-bomb atmospheric calibration curve to the different sample weight sequences, were all significant except for the 200 µgC graphite targets. Our results indicate that samples smaller than 350 µgC have limited accuracy and precision. Overall, reliable measurements of F¹⁴C sequences from tree-ring records across a range of sample sizes, with best results found using graphitized samples >350 µgC.

KEYWORDS: environmental change, F¹⁴C, MIni CARbon DAting System (MICADAS), small sample size, tree rings.

INTRODUCTION

The Chronos ¹⁴Carbon-Cycle Facility (henceforth Chronos) was opened in 2019 and houses an Ionplus MIni CARbon DAting System (MICADAS) for accelerator mass spectrometry (AMS) analysis along with a fully automated Ionplus AGE3 graphitization System (Turney et al. 2021). The facility was designed with the aim of better understanding environmental change, specifically in regions of the world where there are limited long-term (>100 years) instrumental records. The combined AGE3 and MICADAS systems allow for high throughput of samples processed from smaller initial masses of material than other AMS systems (Wacker et al. 2010a). This is especially important for analyzing wood samples where annual tree-ring measurements of F¹⁴C are needed. However, it is possible for tree rings to be very narrow in larger tropical or arid trees, limiting available sample material. Additionally, due to the heavy logging of Australian forests, many of the larger and older trees remain solely in National Parks, where the analysis must be conducted using small-diameter tree cores. Therefore, accessing sufficient sample material to produce a full-sized graphite target (1000 µg of carbon for a MICADAS system) can be challenging. A Gas Interface System (GIS) for the MICADAS is designed for small sample sizes (Wacker et al. 2013). However, smaller-sized tree-ring samples typically have a large enough amount of

*Corresponding author. Email: h.haines@unsw.edu.au

carbon that they can be graphitized to produce a viable target, ranging between 200 and 1000 μgC . Additionally, these narrow rings are often contained within sequences of rings suitable for developing full-sized graphite targets prepared on the AGE3 system. For consistency in analysis, sequences should be measured using the same procedures throughout, which is why it is ideal to only use graphitized targets where possible for wood analysis.

Fortunately, there is precedence for analyzing smaller-sized samples using the AGE3 graphitization system and MICADAS AMS by the Bristol Radiocarbon Accelerator Mass Spectrometry (BRAMS) Facility. Samples containing as little as 200 μg of carbon have been reported to produce reliable measurements when analyzed with size-matched standards and blanks (Knowles et al. 2019). BRAMS utilizes both an AGE3 graphitization and MICADAS system (Knowles et al. 2019), suggesting that it should be possible to analyze targets down to 200 μg of carbon at Chronos. However, Knowles et al. (2019) did not detail the sample type or specific pretreatment used to achieve reliable dates on small samples, other than the need to size-match standards and blanks. To determine the accuracy of F^{14}C measurement of small samples at Chronos, tests were run using modern known-age Australian wood samples of varying size down to 200 μgC targets across the Southern-Hemisphere “bomb peak” of the 1960s (Turney et al. 2018; Hua et al. 2021).

METHODS

A 12-mm-diameter tree core (DMA014E) was subsampled for this study. The core is from a subtropical *Araucaria cunninghamii* tree located in D’Aguilar National Park, Southeast Queensland, Australia and was part of the DMA master tree-ring chronology developed by Haines et al. (2018a). Annual rings for the CE 1962–1970 period were selected as this includes both the sharp rise and fall of the radiocarbon calibration curve surrounding the 1966 bomb spike. This time period spans an extensive range of F^{14}C values so we can best test the sensitivity of the AMS measurements. The nine rings sampled from this core ranged from 1.8 to 10.8 mm wide, with an average width of 6.4 mm. The annual rings were extracted from the core by cutting each ring apart as close to the ring boundaries as possible, while ensuring no overlap between samples. The nine single-ring samples were then chipped into small matchstick-sized pieces perpendicular to the ring-boundaries so that each piece included the entire annual growth period, with approximately 100 mg worth of matchstick pieces used for analysis of each sample. In addition, three 100-mg samples of Manukau kauri (>140,000 years old; Hogg et al. 2006; Marra et al. 2006) were prepared into matchstick-sized pieces and pretreated as ancient wood background samples alongside the nine annual ring samples.

Chemical pretreatment was undertaken at Chronos to transform all raw wood samples and backgrounds into cellulose following a base-acid-base-acid-bleaching (BABAB) method modified slightly from Turney et al. (2021). The samples and ancient wood were first washed three times with 10 mL of acetone, with each wash left for 30 min in a heat block at 55°C. After the three washes, the samples underwent two Milli-Q water rinses. The first base step was then conducted using three 10 mL 1M NaOH base washes for 30 min each in a heat block at 75°C. After the three washes, the samples were again rinsed twice with Milli-Q water. The remaining ABAB steps outlined in Turney et al. (2021) were adapted for processing the larger weight of wood samples (i.e., ca. 100 mg) rather than the reported 10–40 mg sample size noted in Turney et al. (2021). To ensure all the wood was properly

pretreated into cellulose when using these larger weights, the chemical volume was doubled for each chemical processing step, and the bleaching step was extended to 3 hr.

Four different graphite sizes were collected from each of the nine single rings that were pretreated as well as from the three ancient wood background samples. This process was undertaken using a combustion-graphitization system composed of an Elementar vario ISOTOPE select elemental analyzer (EA) and an Ionplus automated graphitization system (AGE3; Wacker et al. 2010b). Iron is used as a catalyst for graphitization and is dispensed using an Ionplus FED dispenser, providing on average 3.9 mg of iron for the catalyzation of each sample. In the EA-AGE3 system, the pure carbon dioxide captured in the graphitization reactor tube is reduced to graphite at 580°C with hydrogen on iron powder. The graphite sizes analyzed included the typical Ionplus factory specified “full” graphitized sample size of 1000 µgC, and the smaller graphitized sample sizes of 500 µgC, 350 µgC, and 200 µgC desired for this study. The EA-AGE3 instrument method is set in the software program for these instruments but it can be modified to capture specific sizes of carbon for graphitization by incrementally reducing the pressure remaining in the graphitization reactor to a determined setpoint. The Chronos EA-AGE3 instrument method was therefore set at the following levels for this study: 570 mbar for 1000 µgC samples, 290 mbar for 500 µgC, and 200 mbar for 350 µgC. To capture 200 µgC samples accurate weights of cellulose needed to be calculated as the EA-AGE3 instrument method was limited to 200 mbar as the minimum reactor pressure setting at the time this experiment was run (an updated Ionplus EA-AGE3 software version now permits lower reactor pressure settings). Cellulose samples were weighed into tin boats with 2.8–3.2 mg of cellulose used for the 1000 µgC samples, 1.54–1.85 mg of cellulose used for the 500 µgC samples, 0.77–1.05 mg of cellulose used for the 350 µgC samples, and 0.513–0.582 mg of cellulose used for the 200 µgC samples. The best practice for selecting cellulose prescribes using an entire matchstick or a portion of matchstick cut smaller lengthwise and representative of the whole ring. However, when collecting cellulose for the smaller 350 µgC and 200 µgC weights, some of the wider rings had matchsticks that needed to be cut smaller crosswise to obtain the desired weight. Where this was undertaken, sampling was performed to capture as much of the annual representation of the ring as possible.

Standards of oxalic acid (OXII, NIST SRM 4990c), IAEA-C8 (oxalic acid, 15.03 ± 0.07 pMC; Le Clercq et al. 1997), and chemical blanks (phthalic anhydride, PhA; SigmaAldrich, PN-320064-10 g) were size matched to produce 1000 µgC, 500 µgC, and 350 µgC of graphite using the mbar levels on the EA-AGE3. All samples, backgrounds, standards, and blanks were pressed pneumatically at 300 MPa into clean aluminium cathodes using an Ionplus press (PSP).

The various-sized graphite samples are produced on a fixed amount of Fe catalyst, resulting in graphitized targets with varying ratios of Fe and C. Three magazines based on sample graphitization size were prepared for routine ^{14}C measurements on the MICADAS; magazine 1 with cathodes containing 1000 µg of carbon, magazine 2 with cathodes containing 500 µg of carbon, and magazine 3 with both the cathodes containing 350 µg of carbon and those containing 200 µg of carbon. The sample graphitization size and the corresponding composition of the graphitized sample produce different C- currents on the MICADAS AMS, thus requiring size-matched samples, backgrounds, standards, and blanks to be measured concurrently in a single magazine of cathodes. The solid graphite

Table 1 Radiocarbon F¹⁴C values for DMA014E as calculated on the Chronos MICADAS.

UNSW lab code	Sample size (µgC)	Year*	F ¹⁴ C value	F ¹⁴ C error†
UNSW-939	1000	1962	1.204	0.004
UNSW-940	1000	1963	1.252	0.004
UNSW-941	1000	1964	1.514	0.004
UNSW-942	1000	1965	1.608	0.004
UNSW-943	1000	1966	1.628	0.004
UNSW-944	1000	1967	1.607	0.004
UNSW-945	1000	1968	1.561	0.004
UNSW-946	1000	1969	1.546	0.004
UNSW-947	1000	1970	1.530	0.004
UNSW-948	500	1962	1.211	0.006
UNSW-949	500	1963	1.243	0.006
UNSW-950	500	1964	1.540	0.006
UNSW-951	500	1965	1.607	0.007
UNSW-952	500	1966	1.630	0.007
UNSW-953	500	1967	1.606	0.007
UNSW-954	500	1968	1.563	0.006
UNSW-955	500	1969	1.551	0.006
UNSW-956	500	1970	1.538	0.007
UNSW-957	350	1962	1.205	0.004
UNSW-958	350	1963	1.281	0.005
UNSW-959	350	1964	1.479	0.005
UNSW-960	350	1965	1.597	0.006
UNSW-961	350	1966	1.628	0.005
UNSW-962	350	1967	1.606	0.005
UNSW-963	350	1968	1.576	0.005
UNSW-964	350	1969	1.548	0.005
UNSW-965	350	1970	1.537	0.005
UNSW-966	200	1962	1.203	0.006
UNSW-967	200	1963	1.289	0.006
UNSW-968	200	1964	1.422	0.006
UNSW-969	200	1965	1.597	0.007
UNSW-970	200	1966	1.619	0.007
UNSW-971	200	1967	1.589	0.006
UNSW-972	200	1968	1.550	0.006
UNSW-973	200	1969	1.542	0.007
UNSW-974	200	1970	1.540	0.006

*Year assigned to each ring is based on dendrochronological analysis.

†F¹⁴C error reported here represents one sigma error.

targets were measured at moderate C- currents (LE), 20–70 µA. Tuning procedures and operating parameters of the MICADAS are described in Turney et al. (2021).

RESULTS AND SUMMARY

The 36 radiocarbon F¹⁴C values obtained from subtropical *A. cunninghamii* tree rings are presented in Table 1 and Figure 1. These values were calibrated using OxCal version 4.4 (Bronk Ramsey 2009) on the SH1-2 post-bomb atmospheric curve (Hua et al. 2013; Hogg

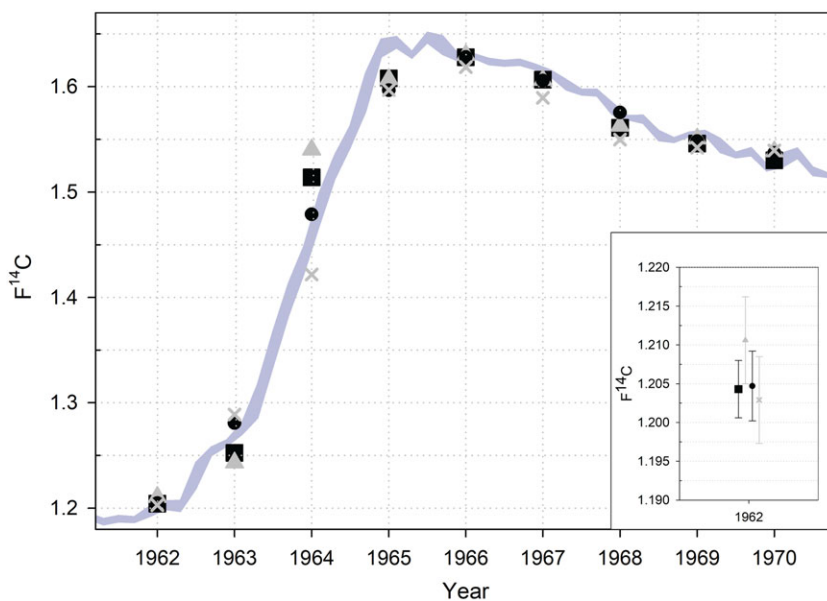


Figure 1 $F^{14}C$ values of the 1962–1970 DMA samples for the 1000 μgC (black squares), 500 μgC (gray triangles), 350 μgC (black circles), and 200 μgC (gray Xs) sized targets as determined on the Chronos MICADAS overlaid on the SH1-2 post-bomb radiocarbon calibration curve (purple line). The inset figure demonstrates the four samples from 1962 offset slightly so as observe their error ranges which are too small to appear on the main image.

et al. 2020). As the age of each ring was already known and confirmed through dendrochronological analysis (Haines et al. 2018a), only the relevant position on either the rising or falling portion of the SH1-2 post-bomb curve was assessed in this study. These results demonstrate that for all four graphite sizes analyzed here, similar $F^{14}C$ values were obtained, which closely follows the Southern Hemisphere post-bomb radiocarbon calibration curve (Figure 1). Samples that rest on flatter portions of the calibration curve demonstrate that the four target sizes either fall within error of each other or come very close to being within error, as can be noted in the inset of Figure 1. However, samples that fall on the steepest part of the calibration curve (CE 1963 and 1964) demonstrate a larger range of values (Figure 1). This reflects the fact that the carbon fixed across these years represents a 7–8-month accumulation period from mid-August to late March (Haines et al. 2018b), during which there were rapid and extreme changes in atmospheric ^{14}C content (Turney et al. 2018). This highlights the need for careful “matchstick” sampling across an entire growth period.

The precision of the $F^{14}C$ results of the different target sizes (Figure 1, Table 1) was assessed by calculating the smaller targets’ paired differences to that of the “standard” 1000 μgC target. The assumption being the paired differences should ideally be zero. For example, the $F^{14}C$ value for the 500 μgC target of 1962 was subtracted from the $F^{14}C$ value of the 1000 μgC sample for the same year. The results are presented in Table 2 and Figure 2 using a Δ (delta) notation to indicate paired differencing. This approach effectively sets up paired sample *t*-test comparisons (McDonald 2014). To test if the paired differences were normally distributed, we used a Shapiro-Wilk test of normality where a threshold of 0.05 indicates a

Table 2 Differences between the $F^{14}C$ values from the smaller-sized samples (i.e., 500 μgC , 350 μgC , 200 μgC) in relation to the full-sized (1000 μgC) samples for each year (indicated using the Δ symbol). The mean and standard deviation (s) of the differences are given. The Shapiro-Wilk test for normality was not passed by the $\Delta 200$ series (value in **bold**), which meant a non-parametric Wilcoxon test (indicated by *) was used instead of the paired t -test for the other two series. The p -values indicate the probability that the values are not significantly different from zero (i.e., $p > 0.05$).

Year	$\Delta 500$	$\Delta 350$	$\Delta 200$
1962	-0.0063	-0.0004	0.0014
1963	0.0092	-0.0282	-0.0364
1964	-0.0263	0.0352	0.0921
1965	0.0008	0.0113	0.0111
1966	-0.0021	-0.0002	0.0093
1967	0.0004	0.0010	0.0173
1968	-0.0018	-0.0145	0.0112
1969	-0.0046	-0.0022	0.0039
1970	-0.0083	-0.0069	-0.0094
Mean	-0.0043	-0.0005	0.0112
s	0.0097	0.0174	0.0343
df (n-1)	8	8	8
Shapiro-Wilk	0.1179	0.4709	0.0214
Paired t -test	-1.3467	-0.0938	33*
p -value	0.2150	0.9275	0.2500

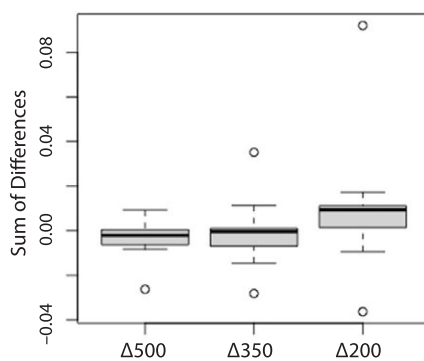


Figure 2 Box and whisker plot of the differences between the 1000 μgC and each of the three smaller-sized graphite targets (i.e., 500 μgC , 350 μgC , 200 μgC). The y -axis represents the sum of the differences in μgC between the full-sized (1000 μgC) targets and the smaller targets noted on the x -axis. The black bar represents the mean, one standard deviation by the shaded box, two standard deviations by the whiskers, and the outliers by the circles.

Table 3 $F^{14}C$ values and target scatter for all oxalic acid (OXII) and IAEA-C8 standards as well as chemical phthalic anhydride (PhA) blanks and Manukau kauri ancient wood backgrounds run on the Chronos MICADAS at the 1000 μgC , 500 μgC , and 350 μgC sizes.

	1000 μgC $F^{14}C$			500 μgC $F^{14}C$			350 μgC $F^{14}C$		
	Average	Std dev	n	Average	Std dev	n	Average	Std dev	n
OXII	1.34063	0.00434	1053	1.34090	0.00270	104	1.34041	0.00349	51
C8	0.15059	0.00111	159	0.14938	0.00180	5	0.15213	0.00379	10
PhA	0.00183	0.00054	299	0.00236	0.00070	34	0.00314	0.00050	13
Manukau kauri	0.00202	0.00059	318	0.00249	0.00060	54	0.00272	0.00038	8

normal distribution. This determined that $\Delta 200$ was skewed and so the non-parametric Wilcoxon test was therefore applied in this instance instead of the paired sample t -test. Overall, the mean of the paired differences for each of the three smaller-sized samples were not significantly different from the 1000 μgC standard, based on statistical test results (Table 2). This means the smaller weight results were of similar precision to that of the conventional sample weight results. However, the skewed (i.e., biased) values for the 200 μgC targets indicate their use must be treated with caution. Some of this error could be from the incomplete sampling of the entire growth ring with larger rings; a risk not normally an issue with a narrow tree ring that only provides enough material for a ~ 200 μgC target. Figure 1 and Table 1 clearly demonstrate that the 200 μgC targets produced $F^{14}C$ values beyond the range of the other samples for wide rings and narrower rings where the entire growth season was sampled, so it would seem other error sources were the cause. It is also known that smaller-sized samples are proportionally affected by any form of chemical or surface contamination during graphitization resulting in a greater possibility of a skewed result (Fahrni et al. 2013). While the use of the Gas Interface System would eliminate some of this contamination due to less handling of a smaller-sized sample, the precision of analysis on the MICADAS is much lower, creating a larger error range for the value provided. Therefore, we believe it is possible to graphitize smaller-sized wood samples as long as greater vigilance is used when analyzing the $F^{14}C$ results.

The capability for analyzing smaller-sized samples was also assessed by looking at the target scatter noted for the backgrounds and standards analyzed in this study at the 1000 μgC , 500 μgC , and 350 μgC sizes producible via carbon capture in the EA-AGE3 system (Table 3). Given the small sample size of this study, the target scatter was calculated for all backgrounds and standards run on the Chronos MICADAS since the facility opened. These values demonstrate that when standard deviation is accounted for, the average $F^{14}C$ values for all standards, blanks, and backgrounds fall within range of each other regardless of target size. The only exception is the 350 μgC sized PhA chemical blanks however, given the small amount of $F^{14}C$ and the fact that any surface contamination on the tin boats used in graphitization, the aluminium cathodes used in the AMS, as well as on the tools used to transfer the graphite will result in proportionally higher backgrounds in both older and smaller samples this value slightly outside of the standard deviation range can be expected. It should also be noted that for the three magazines run for this project, all standards, blanks, and background $F^{14}C$ values fell within the standard deviation of the average values reported in Table 3, with the exception of some of the 350 μgC PhA

cathodes which can be explained by the possibility of contamination noted above. The consistent and comparable results between the different sized standards, blanks, and backgrounds demonstrate the ability of the Chronos MICADAS to normalize and correct the values for samples of all sizes discussed in this study. It is also important to ensure that all samples are run against standards and backgrounds which have been size matched to provide the most comparable analysis (Knowles et al. 2019).

We also tested the accuracy of our $F^{14}C$ measurements against the calibration curve. Using the program OxCal version 4.4 (Bronk Ramsey 2009), each of the four different target weight sequences were calibrated to the Southern Hemisphere region 1-2 (SH1-2) post-bomb atmospheric calibration curve. Our 9-year study period includes, at the start, the steep rise to the bomb peak and this was considered to unduly bias any “wigggle-matching” statistical testing. We therefore selected the shortened window of CE 1966–1970, that is post bomb-spike, to determine how accurate the wigggle-matched sequences (Bronk Ramsey et al. 2001; Hogg et al. 2011) of values were for the four different target weights. The chi-squared analysis results are 65.2, 111.6, 79.4, and 0.6 for 1000, 500, 350, and 200 μgC targets respectively, with all but the 200 μgC target sequence passing the statistical significance threshold. This suggests all samples from 350 μgC upwards represented accurate $F^{14}C$ measurements in relation to the atmospheric calibration curve.

An additional test of the accuracy of the $F^{14}C$ measurements, specifically on the steep upward climb of the bomb-spike, saw us review the four samples from CE 1964, where the greatest variance in $F^{14}C$ can be found in a single year. These values were plotted in OxCal on the SH1-2 post-bomb atmospheric curve and compared to each other (Figure 3). For the 1000 μgC , 500 μgC , and 350 μgC samples, the probable calendar date on the upwards pre-bomb slope as assigned by OxCal was CE 1964 (Figure 3a–c, respectively). For the 200 μgC sample, the most probable calendar date was given as CE 1963; however, as seen in Figure 3d, the suggestion of CE 1963 is based on a spike in $F^{14}C$ at the end of this year, but the probability distribution extends into CE 1964. Given that most analyses of modern wood samples would involve a mixture of radiocarbon dating and dendrochronological analysis, the ability exists for the correct date to be assigned to this ring with all four graphite sample sizes tested here. However, the result for the 200 μgC sample once again illustrates the need for cautious interpretation.

Overall, these results show that Chronos can produce accurate and precise $F^{14}C$ measurements in small-sized wood samples down to 350 μgC through the use of the standard pretreatment, operation, and analysis procedures. However, great care is needed for samples $<350 \mu\text{gC}$ as there is potential for lower accuracy and precision in replicating atmospheric $F^{14}C$. This is particularly important for Australian dendrochronological analysis as tree rings in many species from tropical, arid, and some temperate locations may only provide very small amounts of wood per annual ring. When performing radiocarbon analysis on minimal pieces of wood, or any material for that matter, extra care needs to be taken, as any contamination will have a greater effect on a small sample than a larger one. It should also be noted that this study was undertaken on a modern tree core in good condition. While it is likely that the capability of the facility to measure small graphite targets extends back beyond modern wood samples, further study is needed to confirm such analysis is also applicable to much older samples, samples that have been degraded prior to sampling, or are from another dateable material type (e.g., macrofossils, charcoal, peat).

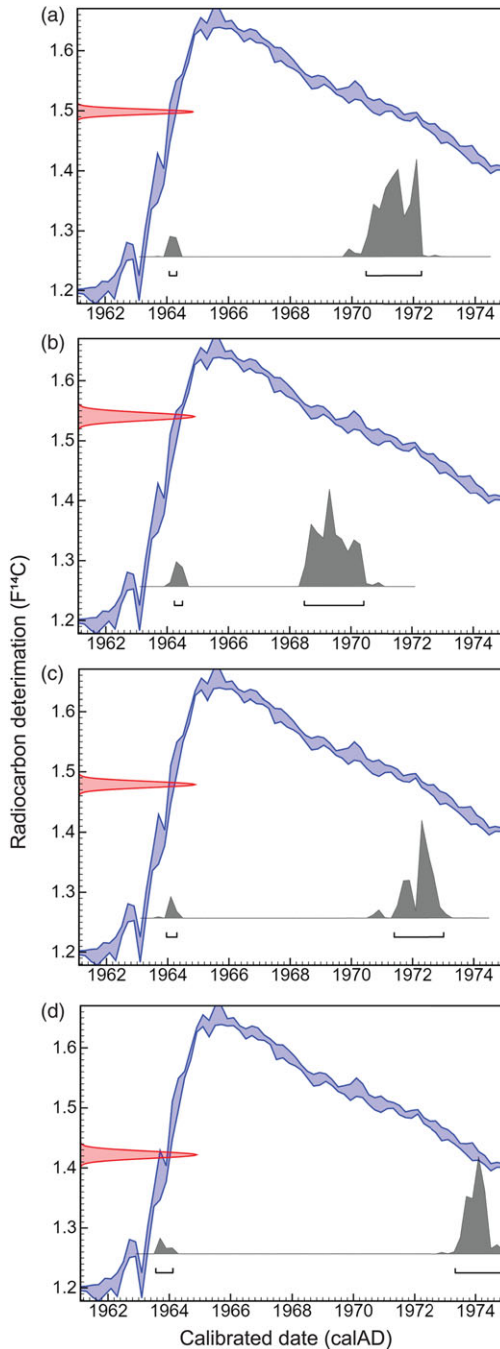


Figure 3 Calibration of the 1964 DMA radiocarbon dates for the range of graphite sample sizes (a) 1000 μgC , (b) 500 μgC , (c) 350 μgC , (d) 200 μgC tested on the Chronos MICADAS. The calibration curve is shown in blue, the $F^{14}\text{C}$ value range for each sample in red and the probable ages in gray. Radiocarbon age calibration was calculated using SH1-2 post-bomb atmospheric curve (Hua et al. 2013; Hogg et al. 2020) and OxCal version 4.4 (Bronk Ramsey 2009).

ACKNOWLEDGMENTS

We would like to thank Chris Bronk Ramsey for his advice on using OxCal to analyze our data. Thanks also to two anonymous reviewers for their comments on an earlier draft of this manuscript.

COMPETING INTERESTS

The authors declare no competing interests exist.

REFERENCES

- Bronk Ramsey C. 2009. Bayesian analysis of radiocarbon dates. *Radiocarbon* 51(1):337–360. doi: [10.1017/S0033822200033865](https://doi.org/10.1017/S0033822200033865).
- Bronk Ramsey C, van der Plicht J, Weninger B. 2001. “Wiggle matching” radiocarbon dates. *Radiocarbon* 43(2A):381–389. doi: [10.1017/S0033822200038248](https://doi.org/10.1017/S0033822200038248).
- Fahrni SM, Wacker L, Synal H-A, Szidat S. 2013. Improving a gas ion source for ^{14}C AMS. *Nuclear Instruments and Methods in Physics Research Section B: Beam Interactions with Materials and Atoms* 294:320–327. doi: [10.1016/j.nimb.2012.03.037](https://doi.org/10.1016/j.nimb.2012.03.037).
- Haines HA, Gadd PS, Palmer JG, Olley J, Hua Q, Heijnis H. 2018a. A new method for dating tree-rings in trees with faint, indeterminate ring boundaries using the Itrax core scanner. *Palaeogeography, Palaeoclimatology, Palaeoecology* 497:234–243. doi: [10.1016/j.palaeo.2018.02.025](https://doi.org/10.1016/j.palaeo.2018.02.025).
- Haines HA, Olley JM, English NB, Hua Q. 2018b. Anomalous ring identification in two Australian subtropical Araucariaceae species permits annual ring dating and growth-climate relationship development. *Dendrochronologia* 49:16–20. doi: [10.1016/j.dendro.2018.02.008](https://doi.org/10.1016/j.dendro.2018.02.008).
- Hogg AG, Fifield LK, Turney CSM, Palmer JG, Galbraith R, Baillie MGK. 2006. Dating ancient wood by high-sensitivity liquid scintillation counting and accelerator mass spectrometry-pushing the boundaries. *Quaternary Geochronology* 1(4):241–248. doi: [10.1016/j.quageo.2006.11.001](https://doi.org/10.1016/j.quageo.2006.11.001).
- Hogg AG, Heaton T, Hua Q, Palmer J, Turney C, Southon J, Bayliss A, Blackwell P, Boswijk G, Bronk Ramsey C, Petchey F, Reimer P, Reimer R, Wacker L. 2020. SHCal20 Southern Hemisphere calibration, 0–55,000 years cal BP. *Radiocarbon* 62(4):759–778. doi: [10.1017/RDC.2020.59](https://doi.org/10.1017/RDC.2020.59).
- Hogg AG, Lowe DJ, Palmer JG, Boswijk G, Bronk Ramsey C. 2011. Revised calendar date for the Taupo eruption derived by ^{14}C wiggle-matching using a New Zealand kauri ^{14}C calibration data set. *The Holocene* 22(4):439–449. doi: [10.1177/0959683611425551](https://doi.org/10.1177/0959683611425551).
- Hua Q, Barbetti M, Rakowski AJ. 2013. Atmospheric radiocarbon for the period 1950–2010. *Radiocarbon* 55(4):2059–2072. doi: [10.2458/azu_js_rc.v55i2.16177](https://doi.org/10.2458/azu_js_rc.v55i2.16177).
- Hua Q, Turnbull JC, Santos GM, Rakowski AZ, Ancapichún S, De Pol-Holz R, Hammer S, Lehman SJ, Levin I, Miller JB, Palmer JG, Turney CSM. 2021. Atmospheric radiocarbon for the period 1950–2019. *Radiocarbon*. doi: [10.1017/RDC.2021.95](https://doi.org/10.1017/RDC.2021.95).
- Knowles TDJ, Monaghan PS, Evershed RP. 2019. Radiocarbon sample preparation procedures and the first status report from the Bristol Radiocarbon AMS (BRAMS) Facility. *Radiocarbon* 61(5):1541–1550. doi: [10.1017/RDC.2019.28](https://doi.org/10.1017/RDC.2019.28).
- Le Clercq M, van der Plicht J, Gröning M. 1997. New ^{14}C reference materials with activities of 15 and 50 PMC. *Radiocarbon* 40(1):295–297. doi: [10.1017/S0033822200018178](https://doi.org/10.1017/S0033822200018178).
- Marra MJ, Alloway BV, Newnham RM. 2006. Paleoenvironmental reconstruction of a well-preserved Stage 7 forest sequence catastrophically buried by basaltic eruptive deposits, northern New Zealand. *Quaternary Science Reviews* 25:2143–2161. doi: [10.1016/j.quascirev.2006.01.031](https://doi.org/10.1016/j.quascirev.2006.01.031).
- McDonald JH. 2014. *Handbook of biological statistics*. 3rd ed. Baltimore (MD): Sparky House Publishing.
- Turney CSM, Becerra-Valdivia L, Sookdeo A, Thomas ZA, Palmer JG, Haines HA, Cadd H, Wacker L, Baker A, Andersen MS, Jacobsen G, Meredith K, Chinu K, Bollhalder S, Marjo C. 2021. Radiocarbon protocols and first intercomparison results from the Chronos ^{14}C Carbon-Cycle Facility, University of New South Wales, Sydney, Australia. *Radiocarbon* 63(3):1003–1023. doi: [10.1017/RDC.2021.23](https://doi.org/10.1017/RDC.2021.23).
- Turney CSM, Palmer JG, Maslin MA, Hogg A, Fogwill CJ, Southon J, Fenwick P, Helle G, Wilmhurst JM, McGlone M, Bronk Ramsey C, Thomas ZA, Lipson M, Beaven B, Jones RT, Andrews O, Hua Q. 2018. Global peak in atmospheric radiocarbon provides a potential definition for the onset of the Anthropocene Epoch in 1965. *Scientific Reports* 8(1):1–10. doi: [10.1038/s41598-018-20970-5](https://doi.org/10.1038/s41598-018-20970-5).
- Wacker L, Bonani G, Friedrich M, Hajdas I, Kromer B, Němec M, Ruff M, Suter M, Synal H,

- Vockenhuber C. 2010a. MICADAS: Routine and high-precision radiocarbon dating. *Radiocarbon* 52(02):252–262. doi: [10.1017/S0033822200045288](https://doi.org/10.1017/S0033822200045288).
- Wacker L, Fahrni SM, Hajdas I, Molnar M, Sýnal HA, Szidat S, Zhang YL. 2013. A versatile gas interface for routine radiocarbon analysis with a gas ion source. *Nuclear Instruments and Methods in Physics Research Section B: Beam Interactions with Materials and Atoms* 294: 315–319. doi: [10.1016/j.nimb.2012.02.009](https://doi.org/10.1016/j.nimb.2012.02.009).
- Wacker L, Němec M, Bourquin J. 2010b. A revolutionary graphitization system: Fully automated, compact and simple. *Nuclear Instruments and Methods in Physics Research B*, 268(7–8):931–934. doi: [10.1016/j.nimb.2009.10.067](https://doi.org/10.1016/j.nimb.2009.10.067).